

# We are IntechOpen, the world's leading publisher of Open Access books Built by scientists, for scientists

6,900

Open access books available

185,000

International authors and editors

200M

Downloads

Our authors are among the

154

Countries delivered to

TOP 1%

most cited scientists

12.2%

Contributors from top 500 universities



WEB OF SCIENCE™

Selection of our books indexed in the Book Citation Index  
in Web of Science™ Core Collection (BKCI)

Interested in publishing with us?  
Contact [book.department@intechopen.com](mailto:book.department@intechopen.com)

Numbers displayed above are based on latest data collected.  
For more information visit [www.intechopen.com](http://www.intechopen.com)



# Electrochemical Investigation of Porphyrin and Its Derivatives at Various Interfaces

Xiaoquan Lu and Samrat Devaramani

Additional information is available at the end of the chapter

<http://dx.doi.org/10.5772/67637>

## Abstract

This chapter describes the electrochemistry of the porphyrins at solid-liquid and liquid-liquid interfaces. The fundamental electrochemical approach toward the porphyrin molecules in estimating their HOMO and LUMO energy levels is given. Various factors such as the effect of central metal ion, the periphery of the aromatic ring and axial ligands on the redox potentials of porphyrins have been discussed. Electrochemical sensing application of porphyrin molecules is described with few examples in brief. Much focus has been given on the electrochemistry of the self-assembled monolayer (SAM) of thiol-porphyrins on the gold electrode. Structural characterization and charge transfer across the SAM using cyclic voltammetry and electrochemical impedance spectroscopy are discussed. Theory and methodologies developed to study photoinduced charge transfer kinetics of porphyrin molecules using scanning electrochemical microscope at the solid-liquid and liquid-liquid interface have been described. Use of porphyrin molecules as lumino-phores in electrochemiluminescence sensing applications and the mechanisms involved are described through representative examples.

**Keywords:** porphyrin, electrochemistry, interface, SECM, ECL

## 1. Introduction

In the natural photosynthesis process, chlorophyll converts incident light into chemical energy with nearly 100% quantum yield through many complex steps. This excellent phenomenon inspired many scientists to study porphyrin derivatives and their metallated forms extensively for many decades and continue to be so. Substantial information has been gathered on the synthesis, structural characterization, and dependence of their property on the structure and applications of porphyrins [1]. Porphyrins can be tailored by modifying the aromatic

ring at the  $\beta$  and *meso* positions of the pyrrole and by metallating the tetradentate core of the porphyrin ring with almost all the transition metal ions. Thereby electronic properties of the porphyrins such as redox process, light absorption property, energy, and electron transfer capabilities can be amended [2]. Hence, porphyrins have witnessed their participation in the wide range of applications in various fields such as photovoltaics, artificial photosynthesis, photodynamic therapy, catalysis, and enzymatic systems.

As mentioned above, crafting the redox potentials of the porphyrins by modifying the periphery or the core of the aromatic ring remains the key strategy behind its multifunctional behavior. Most of such compounds are electroactive, exhibit multiple redox couples, and have been investigated for their electrochemical properties, generally, in nonaqueous solvents. Various factors such as a type of metal ion and its oxidation state present at the core, nature of the macrocyclic aromatic ring, and an axial ligand attached to the metal ion will affect the electrochemistry of the molecule.

Porphyrins exhibit outstanding absorption of electromagnetic radiation in the visible region. Upon light illumination, electrons present in the HOMO will get excited to LUMO of the porphyrin. Photoexcitation followed by various relaxation processes and charge separation is shown in **Figure 1**. Long-lived radical ion pairs of porphyrins can be observed by stabilizing the charge separated states. Generally, the basic electrochemistry of the porphyrins is related to its electron donating or accepting behavior in the ground state. Electrochemistry of porphyrins under conditions similar to that of photovoltaic devices, artificial photosynthetic systems involves the other states depicted in **Figure 1**. In the following sections, we discuss the fundamental and applied electrochemistry of the porphyrins and its derivatives. Without going for the exhaustive citation of all the reported literature, representative examples have been chosen to support our discussion.

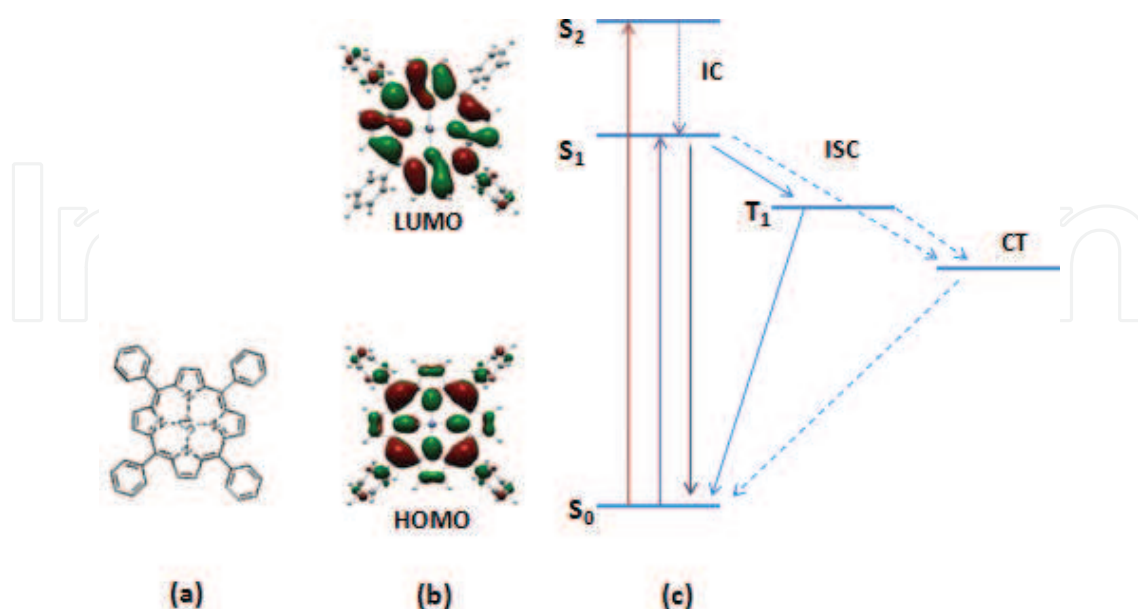


**Figure 1.** Representation of the molecular structure (a), HOMO and LUMO (b) of zinc tetraphenylporphyrin (ZnTPP) and the photoexcitation process followed by various relaxation events (c). Reprinted with permission from Ref. [65]. Copyright 2015 Elsevier Ltd.

## 2. HOMO and LUMO energy levels of porphyrins

Electrochemical techniques such as cyclic voltammetry and differential pulse voltammetry are generally used to estimate the HOMO and LUMO energy levels of the organic compounds. Oxidation onset potential, that is, the energy required to take out the first electron from the HOMO of the molecule will give the HOMO energy level of the molecule under study in eV versus the reference electrode used. In a similar way, reduction onset potential, that is, the energy required to add the first electron to LUMO of the molecule will give information about the energy level of the LUMO of the molecule. Ferrocene (Fc) or other common references used as an internal standard to complete the calculation by using following equations. Such electrochemical studies generally carried out in organic solvents with a suitable electrolyte.

$$E_{\text{HOMO}} = -(E_{\text{onset}}^{\text{ox}} + E_{1/2} \text{ of reference}) \text{ (eV)} \quad (1)$$

$$E_{\text{LUMO}} = -(E_{\text{onset}}^{\text{red}} + E_{1/2} \text{ of reference}) \text{ (eV)} \quad (2)$$

By knowing HOMO and LUMO energy levels, one can calculate the energy gap ( $E_g$ ) between them.

### 2.1. Effect of metal ion

Cheng et al. calculated the HOMO and LUMO energy levels of the tetraphenylporphyrin (TPP) and Cu, Zn, Ni, Pd, and Pt metallated porphyrins (MTPP) [3]. Cyclic voltammograms (CVs) were recorded for TPP and MTPP in acetonitrile using tetra-n-butylammonium hexafluorophosphate as an electrolyte. Quinoxalinoporphyrin and its zincated form were studied in chlorobenzene with tetrabutylammonium tetrafluoroborate as an electrolyte versus Fc/Fc<sup>+</sup> by recording the CVs.  $E_g$  values calculated from the electrochemical method were comparable to those obtained from the electronic spectra [4]. In both the examples mentioned above, expected change in the energy levels of HOMO and LUMO of the porphyrin molecules after metallation was obtained in the electrochemical results. A linear relationship between the electronegativity of the divalent central metal ion and the first ring-centered oxidation and reduction potential was observed [5].

### 2.2. Effect of modifying the periphery of aromatic ring

Factors such as electron donating or withdrawing nature of the substituent, where it has been located on the ring and its number will affect the oxidation and reduction potentials. Influence of  $\pi$ -extension of the aromatic ring on the electrochemistry has been reported for platinum (II) porphyrin derivatives [6]. Dependence of the oxidation and reduction half-wave potentials of the porphyrins on the planarity of the molecule has been discussed by Shelnutt et al. in their review with various examples [7].

### 2.3. Effect of axial ligand

Coordination of nitrogenous bases is generally used in the axial ligation of metalloporphyrins. Type of ligand participated in the axial ligation can manipulate the oxidation and reduction

half-wave potentials of the metalloporphyrins. Kadish et al. have discussed this in detail with exemplifying a large number of ligands possessing nitrogen as a donor atom with iron and cobalt porphyrins [8]. Basic electrochemistry of metalloporphyrins has been discussed in detail with numerous examples by Kadish et al. in a series of book volumes and also in reviews [9].

### 3. Porphyrins at solid-liquid interface

#### 3.1. Sensors

Because of the multifunctional property and their interaction with the various analyte molecules, porphyrins deliver different signal outputs. Porphyrin molecules have been used for sensing applications through optical, electrochemical, different spectral modes. Electrochemical sensing methods developed using porphyrin molecules by our group is discussed here briefly. Porphyrin monolayer was used to electrochemically sense the phosphate anion based on the hydrogen bonding interaction. Upon hydrogen bonding of  $\text{PO}_4^{2-}$  with  $-\text{NH}$ , ease of charge transfer between the redox mediator and monolayer on the electrode was increased. Taking the advantage of this, decrease in the charge transfer resistance,  $R_{\text{ct}}$  and increase in the magnitude of the normalized current of the approach curves recorded by SECM were measured to sense the phosphate anion [10]. The same strategy has been used to quantify the porphyrin molecules in the pheophytin samples obtained from the spinach leaves. In this method, a gold electrode was modified with phosphate monolayer and used for the electrochemical sensing of porphyrin.  $R_{\text{ct}}$  value with increased concentration of porphyrin was found to be linear in the  $1.0 \times 10^{-7}$  M to  $5.0 \times 10^{-5}$  M concentration range. The detection limit,  $3.0 \times 10^{-8}$  M was superior to that of an optical method which was parallelly done [11]. The electrochemical sensing of m-dinitrobenzene (m-DNB) was demonstrated based on the same concept. Hydroxyl group(s) present at the periphery of the porphyrin ring form hydrogen bond with the nitro group of the m-DNB. Further, the benzene ring of the analyte will orient parallel to the macrocyclic  $\pi$ -ring of the porphyrin to result in the charge transfer interactions. As expected, increase in the number of hydroxyl groups on the porphyrin ring lead to the improved differential pulse stripping voltammetric analytical signal [12]. Taking the advantage of hydrogen bonding and  $\pi$ - $\pi$  interaction between the analyte molecules and porphyrin macrocyclic ring, simultaneous determination of hydroquinone (HQ), catechol (CA), and resorcinol (RC) was proposed using 5,10,15,20-tetrakis(4-hydroxyphenyl)porphyrin (THPP)-CNT composite. HOMO and LUMO levels of the three analytes calculated from the density functional theory. HOMO energy level of the hydroquinone found to be highest and that of resorcinol is least. It is understood that higher the energy level of HOMO, it is easier to oxidize the molecule. The strength of the hydrogen bonding, an extent of  $\pi$ - $\pi$  interaction between the THPP and the three analytes is different due to a difference in the charge distribution. Hence the affinity and oxidation potentials of the HQ, CA, and RC on the THPP-CNT-modified electrode resulted in the well-separated and sensitive peaks (**Figure 2**) which are not possible in case of bare and CNT-modified electrode [13]. Composites of porphyrin with carbon substrates such as graphene and fullerene have been reported for the electro and photoelectrochemical sensing of hydroquinone and m-DNB [14, 15].



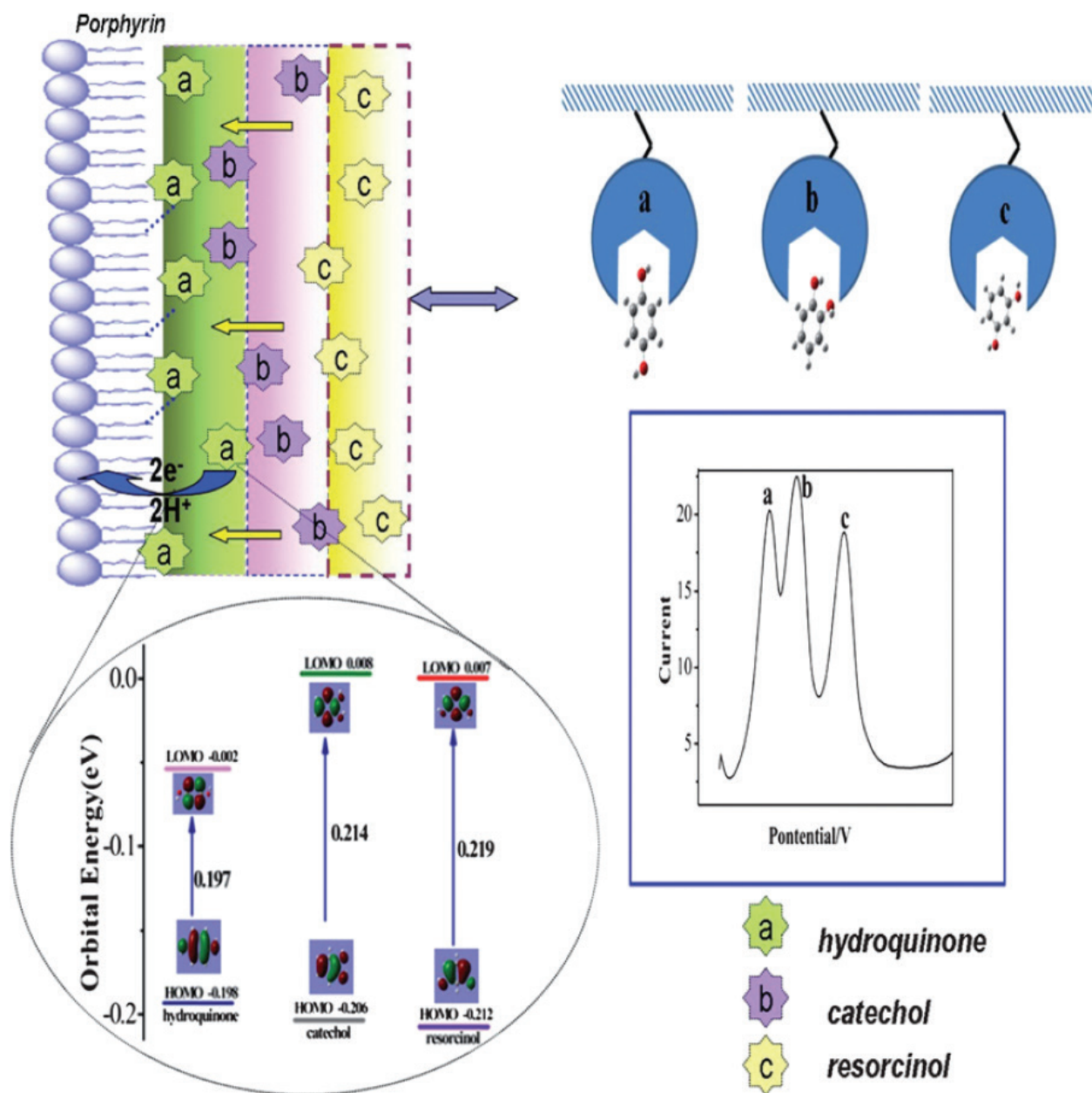


**Figure 2.** Representation of the density of the electron atmosphere of the dihydroxybenzene isomers and the interaction between porphyrin and dihydroxybenzene isomers. Adapted from Ref. [13] with permission from The Royal Society of Chemistry.

### 3.2. Monolayers of porphyrin derivatives

Organosulfur compounds are well studied for the formation of self-assembled monolayers (SAMs) on the gold substrate. SAMs have been studied for their effect on the interfacial properties. A molecule which involved in the formation of SAM can be divided into three parts. Head group of the molecule will interact with the gold substrate, a free end of the molecule can be considered as a tail group and the thickness and structure of the SAM will be decided by the spacer or linker moiety present between the head and tail. SAMs provide an ideal system

for the electrochemical study of heterogeneous charge transfer. Effect of the length of linker molecule on the adsorption kinetics of 5-[*p*-(mercaptoalkoxy)-phenyl]-10,15,20-triphenylporphyrin molecules denoted as  $H_2TPPO(CH_2)_nSH$  was studied by varying the  $n$  from 3 to 12 [16]. Cyclic voltammetry and electrochemical impedance spectroscopy were used to observe the time dependence of the surface coverage and orientation of  $H_2TPPO(CH_2)_nSH$  on the gold electrode. Adsorption rate constant was found to decrease with the increase in the length of the linker molecule. Though the bulky porphyrin molecules are present at the terminal, adsorption steps were similar to that of bare alkanethiols. The monolayers formed as a result of interaction between thiol and gold substrate are compact. Still, there will be imperfections in the form of pinholes. Hence, molecules or ions will reach electrode surface through them to result in a charge transfer. Hence, it is important to have information about such imperfections. The same set of different alkyl length thiol-porphyrin molecules was used to study the surface coverage, size, and distribution of pinholes present in the monolayer. The size of the pinholes estimated using EIS was ranged between 4 and 6  $\mu M$  with 40–70  $\mu M$  separation between them. Randles equivalent circuit and pore size distribution model were used in the analysis of monolayer structure [17]. Electrocatalytic activity of the metalloporphyrins depends on their orientation in the film produced on the electrode [18, 19]. Cobalt tetraphenylporphyrin (CoTPP) monolayers were prepared on the gold electrode using two different linker molecules such as a 3-mercaptopropionic acid (MPA), 4-mercaptopyridine (MPY). Free base porphyrin, tetra-[*p*-(3-mercaptopropoxy)-phenyl]-porphyrin (TMPP) was first assembled to result in monolayer and then metallated with cobalt. The orientation of the porphyrins with respect to a gold electrode in all the three cases was different. Further, the second layer of CoTPP was prepared using imidazole as an axial ligand. Effect of orientation of porphyrin molecules in SAMs on the dioxygen reduction was studied in perchloric acid. Mono- and multi-layers of CoTPP prepared using MPY exhibited the highest catalytic activity [20]. The cofacial arrangement of porphyrins on the electrode found to be more effective for oxygen reduction [21, 22]. Electron transfer across the thiol-TTP and thiol-CoTPP monolayers was examined on a gold electrode in the aqueous solution. Direct electron transfer was blocked when the compact monolayer of the thiol-porphyrin was present. With the decrease in the density of the thiol-porphyrin in the monolayer, electron transfer was observed. Different potentials were applied to promote the charge transfer across the monolayer and the electron transfer rate constants were calculated using the cole-cole plot [23].

Generally, porphyrin monolayer formed by assembling each porphyrin molecule on the gold electrode through one thio- or thioacetate-group, that is, through one clip. Studies on the formation of SAMs using multi clips are seldom [24, 25]. Our group investigated the formation of SAM of tetra[*p*-(3-mercaptopropoxy)phenyl]porphyrin ( $PPS_4$ ) with four clips. Dense SAM was formed in the case of porphyrins with four clips compared to that with one clip. Charge transfer through the SAM by tunneling mechanism and the thickness of the films were taken into consideration to propose the arrangement of porphyrin molecules in the SAM. Considering the arrangement of porphyrins as shown in **Figure 3**, the thickness of the porphyrin film in the case of four clips should be less compared to that of one clip. Therefore greater tunneling current can be expected in the case of four clipped porphyrins. But the contradictory electrochemical results were observed, hence the arrangement of porphyrins with four clips was proposed as shown in **Figure 3d**. Gold electrode modified with the  $PPS_4$  monolayer can behave as nanometer scaled photoswitches [26].

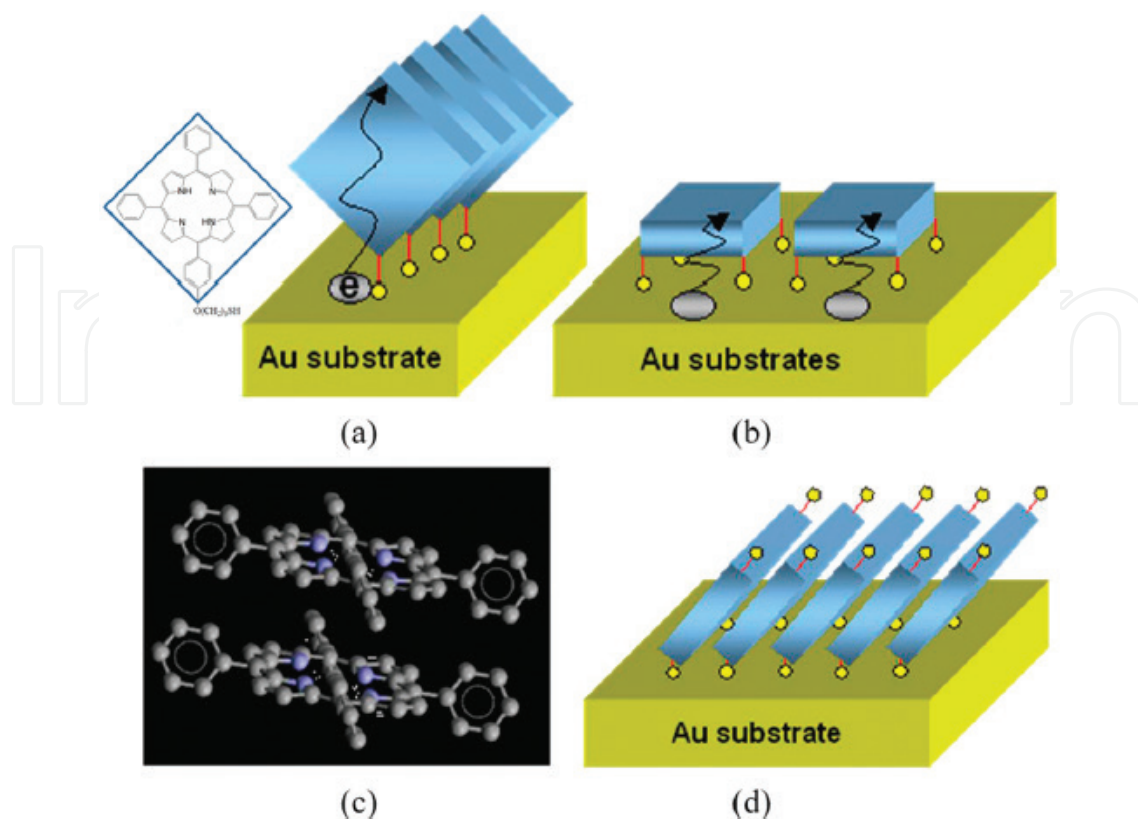


**Figure 3.** Representation of the possible arrangement of porphyrin molecules bearing one clip (a) and four clips (b and d) to form SAM on Au Surface. Skeletal structures of the porphyrin molecules (c). Adapted with permission from Ref. [26]. Copyright 2010 American Chemical Society.

A monolayer of base porphyrin 5-[p-(mercaptopropoxy)-phenyl]-10,15,20-triphenylporphyrin,  $H_2MPTPP$  and its Co and Ni metallated forms were produced on the gold electrode to study their interaction with the DNA at the electrode/electrolyte interface. The magnitude of interaction was understood by calculating the heterogeneous rate constant values from SECM and EIS. Electrostatic attraction between DNA and Ni-MPTPP found highest and it was least in the case of  $H_2MPTPP$  [27]. Based on the strong interaction between iron porphyrin and DNA, a composite film prepared out of this combination was used for electrochemical sensing of p-nitrophenol [28].

Moving on from electrochemical properties of a monolayer of porphyrins, multilayered films were constructed. Gold nanoparticles (AuNPs) and 5,15-di-[p-(6-mercaptohexyl)-phenyl]-10,20-diphenylporphyrin (trans-PPS<sub>2</sub>) were used as inorganic and organic materials, respectively, to form hybrid multilayer film on the gold electrode. Electrochemical property particularly heterogeneous charge transfer constant,  $k_{eff}$  was deduced at different stages of multilayer formation using EIS and SECM. Irrespective of the number of layers on the gold electrode, the material present at the film/electrolyte interface influence the charge transfer resistance of the multilayer. Low charge transfer resistance was observed when the AuNPs are present as the final layer, whereas the trans-PPS<sub>2</sub> at the interface resulted in the high charge transfer resistance. SECM images were recorded by exposing the AuNPs or trans-PPS<sub>2</sub> to the interface. In the case of AuNPs' layer at the interface greater extent of normalized current



was seen compared to that of trans-PPS<sub>2</sub> confirmed the charge transfer blocking behavior of porphyrin layers. As a conclusion, charge transfer between the gold electrode and the AuNPs decrease with the increase in a number of layers of trans-PPS<sub>2</sub> between them [29].

### 3.3. SECM

So far, electrochemistry of porphyrin molecules at the solid-liquid interface studied using basic techniques such as CV and EIS was discussed. Deducing charge transfer constants using CV is simple and straightforward. But, the factors such as resistive potential drop and double-layer charging current pose an ambiguity on the reliability of the results obtained. SECM measures the steady state current using micro- or submicro-size of the tip. Hence, the measured current will also be very small that in turn minimizes the influence of resistive potential drop and double-layer charging current. Hence, SECM emerged as a versatile experimental technique to study the adsorption kinetics of films on various substrates, charge transfer kinetics across the thin films [30, 31]. Very few studies have also been reported on the investigation of porphyrin films using SECM [32, 33]. Understanding and optimizing the long-range charge transfer across the nanometer thickness films is of prime technological importance in various research fields. Theoretical and experimental approaches have been developed to study such cases using SECM [34].

SAMs of thiol-porphyrins, H<sub>2</sub>TPPO(CH<sub>2</sub>)<sub>n</sub>SH with varied alkyl chain length were formed on the gold electrode to investigate the electron transfer between the electrode and the redox mediator, [Fe(CN)<sub>6</sub>]<sup>3-</sup> present in the electrolyte. Three pathways for the electron transfer were proposed. (I) Mediated electron transfer, in this case, product formed at the tip will be regenerated by the bimolecular reaction. That is the film is also redox active. (II) Tunneling through the film, in this case, film is electro-inactive. Hence, the product formed at the tip of the SECM is regenerated at the electrode by tunneling through the film. (III) Imperfections of the SAM such as pinholes and defects give a way for charge transfer. Theoretical approximations were deduced for all the three situations to calculate the SECM tip current. Experimental approach curves were recorded for the SAMs of different thickness and fitted with the theoretically simulated curves to extract the heterogeneous charge transfer constant,  $k_{\text{eff}}$  values for all the three cases. SECM investigation of the electron transfer in porphyrin systems through the bimolecular process closely resembles the charge transfer in photosystem II [35]. Highly ordered monolayers can be obtained by first assembling the alkanethiols on the gold electrode as a template then introducing the porphyrin molecules on to it. When the alkanethiols were used as templates, the surface coverage of the electrode and electron transfer significantly altered. Also, porphyrin molecules stood perpendicular to the electrode.  $k_{\text{eff}}$  value was significantly improved after introducing the cobalt ions into free porphyrin bases of such monolayer [36]. Electroactive zinc porphyrin films were produced on the transparent electrode by electropolymerization using the bipyridinium as a pendant molecule between the two molecules. The permeability of the film and the charge transport within the film was studied under conditions similar to photovoltaic devices. Four different organic redox mediators were used to record the approach curves. Lateral charge transportation between the adjacent redox active sites was also probed [37]. Micropatterning of transparent electrodes (substrate) was done

using zinc porphyrin molecular squares to produce a film composed of meso- and microporous material. SECM was used to study the molecular sieving and permeability of these films. Cavity size of the sieves was controlled by modifying the porphyrinic squares and the permeability was examined by using the redox mediators with smaller in size compared to that of the cavity. It was observed from the results that the steric property of the redox ion needed for charge compensation also played a significant role in deciding the permeability of the redox species in addition to its size. SECM tip current is observed only if the redox mediators generated at tip successfully accesses the underlying substrate through the cavity of the film and diffuse back to the tip. Based on this substrate generation/tip collection mode of the SECM, imaging of the film was done to understand its sieving ability [38]. Complete removal of thiol-porphyrin SAMs from the electrode is also as important as producing the perfect SAMs to get the clean electrode surface. It is difficult to mechanically wash off the SAMs from the electrode surface. But it can be done electrochemically by applying the sufficient negative potential to the modified electrode [39].

In all the above examples, the charge transfer across the porphyrin film/electrolyte interface was originated as a result of the applied potential. But, the photo-excitation of the porphyrins followed by charge transfer in the dyads and triads systems is well known and widely adopted for the construction of photovoltaic devices and artificial photosynthetic systems. Hence, a model system to study the photoelectrochemical properties of the porphyrin molecules is of prime importance. Our group proposed a novel experimental methodology to study the photoinduced charge transfer kinetics of the porphyrin films using SECM [40]. Porphyrin coated on the transparent electrode will be excited by illuminating light from the bottom to result in the porphyrin cation. The reduced form of the redox mediator at the SECM tip will diffuse toward the film and reduce the porphyrin cation back to its original form by undergoing oxidation. Redox mediator oxidized at the film will travel back to the tip, thereby diffusion cone of redox mediator was generated between the SECM tip and porphyrin-coated electrode (**Figure 4**). Hence, the tip current was increased as it moves close to substrate, that is, positive feedback. Through this bimolecular reaction, SECM tip was used to capture the photoinduced charge by performing the probe approach curve experiment. Such diffusion cone does not form when the light was not illuminated according to the above mechanism. Therefore, negative feedback was obtained when the probe approach curve was recorded (**Figure 5**).

Theoretical equations were proposed for tip current ( $I_T$ ) to fit the experimentally obtained approach curves to directly extract the  $k_{\text{eff}}$  values [41].

$$I_T^k = I_S^k \left( 1 - \frac{I_T^{\text{ins}}}{I_T^{\text{cond}}} \right) + I_T^{\text{ins}} \quad (3)$$

$$I_S^k = \frac{0.78377}{L \left( 1 + \frac{1}{\Lambda} \right)} + \frac{0.68 + 0.3315 \exp\left(\frac{-1.0672}{L}\right)}{1 + \left(\frac{11}{\Lambda + 7.3}\right) / (110 - 40L)} \quad (4)$$

Where,  $I_T^{\text{ins}}$  and  $I_T^{\text{cond}}$  denote the tip current in case of insulating and conducting substrates, respectively. In this case, the transparent electrode is a conducting substrate, hence

$$I_T^{\text{cond}} = 0.68 + \frac{0.78377}{L} + 0.3315 \exp\left(\frac{-1.0672}{L}\right) \quad (5)$$

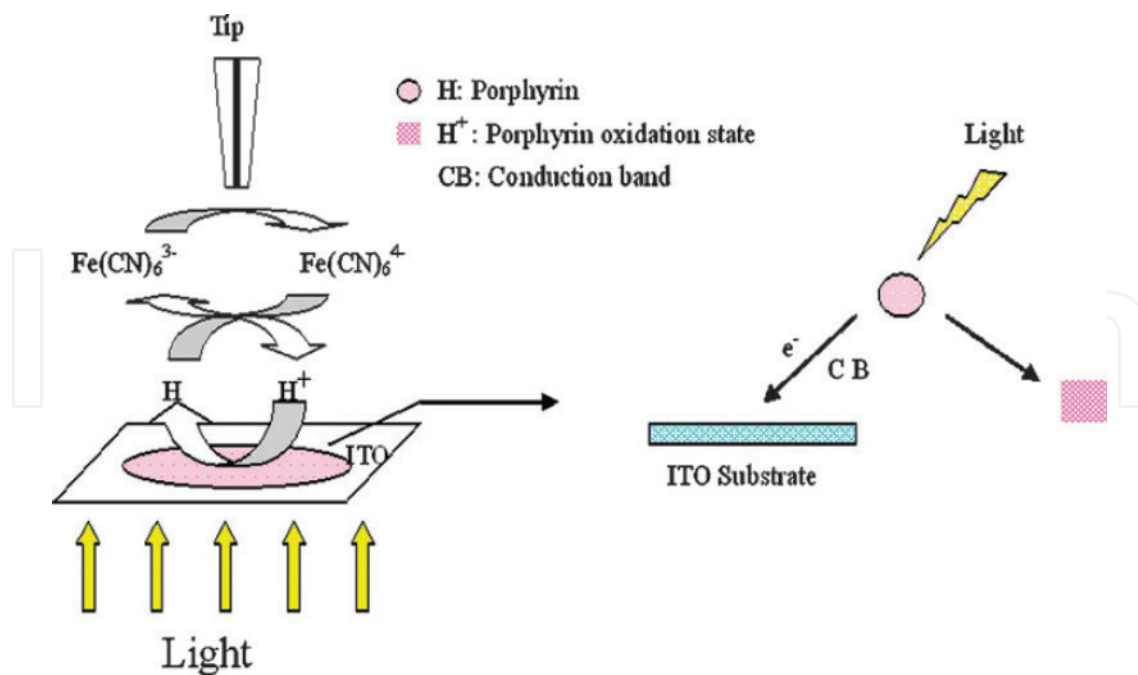


**Figure 4.** Cartoon represents the photoinduced excitation of porphyrin coated on the transparent electrode followed by the bimolecular reaction due to the presence of tip reduced species. Adapted from Ref. [40] with permission from The Royal Society of Chemistry.

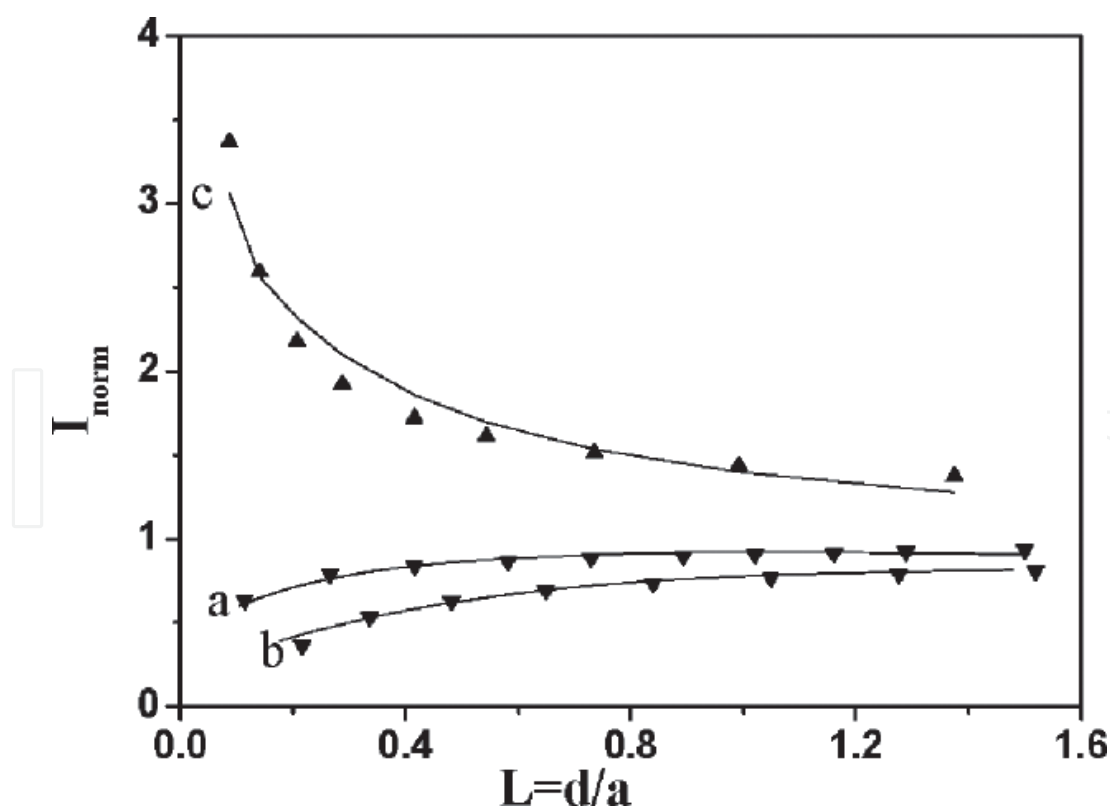


**Figure 5.** Experimental probe approach curves (dotted lines) fitted with the theoretical ones (solid lines) for bare ITO electrode (a), ITO coated with porphyrin in the absence of light (b) and in the presence of light (c). Adapted from Ref. [40] with permission from The Royal Society of Chemistry.

where  $\Lambda = \frac{d k_{\text{eff}}}{D}$ ,  $k_{\text{eff}}$  is the heterogeneous charge transfer constant,  $d$  is the radius of the electro-active part of the SECM tip and  $D$  is the diffusion coefficient of the mediator used. One will arrive with the value of  $\Lambda$  after fitting experimental approach curves with theoretical ones. Then by substituting the value of  $d$ ,  $D$  and  $\Lambda$  in the above equation  $k_{\text{eff}}$  ( $\text{cm s}^{-1}$ ) value can be obtained.

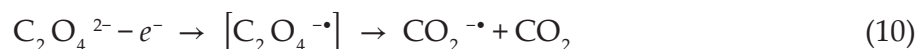
Above methodology was adopted to study the influence of various parameters on the PCT kinetics of zinc porphyrin across the solid/liquid interface using benzoquinone (BQ) as a redox mediator. The family of approach curves was recorded by varying the parameters such as wavelength, the intensity of the light source and for the different concentration of the mediator. The favorable condition for the PCT resulted in the greater  $k_{\text{eff}}$  value [42]. A simple model was constructed using the combination of AuNPs, porphyrin and CNT to mimic the natural photosynthesis system. Core-shell structured composite of AuNP-porphyrin was adsorbed on the vertically aligned CNT on the ITO electrode. The presence of AuNPs at the center of the vesicle structure diminishes the recombination of photogenerated charges and facilitates interfacial charge transfer. CNTs will successfully transfer the received electrons to ITO electrode. These effects were photoelectrochemically studied by recording the approach curves using benzoquinone as a redox mediator. PCT kinetics of this model was found to be dependent on the concentration of electrochemically active benzoquinone. This behavior resembles the role of plastoquinone in natural photosynthesis [43]. Porphyrin molecules loaded on the  $\text{TiO}_2$  nanowire array grown on the ITO electrode by hydrothermal method. Then, change in the PCT kinetics with respect to the length of nanowire array was tested using SECM. With the increase in the length of the nanowire,  $k_{\text{eff}}$  value also becomes greater, may be due to greater amount porphyrin loading [44].

#### 4. Electrochemiluminescence (ECL) of porphyrin

Electrochemiluminescence (ECL) involves a conversion of electrical energy into radiative energy. Fundamental principles, various luminophore systems, applications, and recent advances of ECL have been discussed in detail elsewhere [45, 46]. Polypyridyl complexes are the excessively studied luminophores so far. Because of the rich photo and electrochemical properties, porphyrins have also been used as luminophores in ECL. There are two well-established mechanisms through which ECL can be produced. First one is the annihilation mechanism: In this, a potential of the electrode alternatively pulsed between the two values to produce the oxidized and reduced species of the luminophore. These electrogenerated species at the vicinity of the electrode will interact with each other to produce the excited species, which will return back to the ground state by emitting the radiation [47].



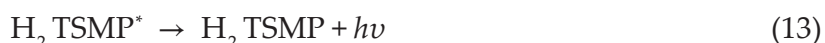
Another way of generating the ECL is by coreactant mechanism: in this, coreactant species upon oxidation or reduction will generate an intermediate, which will further react with the luminophore to cause the excitation. For example, oxalate ion upon oxidation produces the strong reductant. Hence, it is also called as “oxidative-reductive” coreactant [48].



ECL luminophore present in the system also undergoes oxidation at the same potential. For example, tetrakis(3-sulfonatomesityl)porphyrin ( $\text{H}_2\text{TSMP}$ ) [49].



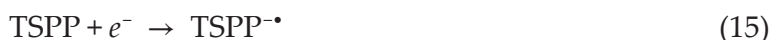
Then the reaction takes place between the oxidized porphyrin and  $\text{CO}_2^{\cdot-}$  produced from the coreactant to result in the excited porphyrin, which will emit radiation.



There is another category of coreactant referred to as “reductive-oxidative,” that is, reduction of the coreactant will produce the strong oxidant species. Peroxydisulfate ( $\text{S}_2\text{O}_8^{2-}$ ) can be mentioned as an example.



Let us consider luminophore, meso-tetra(4-sulfonatophenyl)porphyrin (TSPP) which is also undergoing reduction to produce radical anion under the same conditions [50].



Based on the above mechanisms, ECL sensors have been developed from our group to quantify pheophorbide,  $\text{Cu}^{2+}$ , meso-tetra(4-carboxyphenyl) porphyrin [50–52]. ECL behavior of ruthenium and zinc porphyrins has been electrochemically investigated [53, 54]. Different porphyrin molecules have been studied in combination with clay, carbon nitride, and graphene to improve the intensity of the ECL signal and to achieve the applicability [55–57].

## 5. Porphyrins at liquid-liquid interface

Investigation of the charge transfer process at the liquid-liquid interface, that is, interface between the two immiscible electrolytes (ITIES) has got significance because of its mimicking nature of various fields such as phase transfer catalysis, biomembranes, and drug delivery systems. One of the important outcomes from ITIES studies is the dependence of charge transfer on the driving force. Three important charge transfer processes have been studied at the ITIES.



- Ion transfer
- Electron transfer across the ITIES
- Ion transfer across the ITIES facilitated by the complexing agent

More detailed information about theory, techniques used to study, and applications of ITIES have been discussed in detail in the review by Pekka and Hubert [58]. Generally, in ITIES system, one out of the two phases will be rich of redox species and can be considered metal-like. The potential drop across the ITIES is referred to as the difference of the Galvani potentials of the organic and aqueous phases,  $\Delta_{\omega}^{\circ} \varnothing$ . At low overpotentials, the exponential dependence of electron transfer (ET) rate constant on the  $\Delta_{\omega}^{\circ} \varnothing$  can be expected (Butler-Volmer theory). Whereas at very high overpotentials, the ET rate constants will level off to follow Marcus theory [59].

The theory has been developed to split the complex multistep ET reaction into several one-step processes and the ET rate constant of each step can be calculated. Taking  $\text{ZnTPP}/[\text{Fe}(\text{CN})_6]^{4-}$  as a model system, effect of concentration of the species in the two phases, a thickness of the thin layer on the multistep ET processes was studied using thin layer cyclic voltammetry (TLCV). Experimentally obtained results were found to be in good correlation with the theoretical simulations [60]. Owing to the close resemblance of iron porphyrin with the heme, ET kinetics of the various substituents bearing iron porphyrin was studied by constructing the artificial membrane in the form of ITIES (**Figure 6**). Effect of substituent with different electron affinity on the ET kinetics was understood by recording the approach curves using SECM. Good agreement between the experimentally obtained rate constant values and the electronic structure and molecular orbital energies calculated by the density functional theory was observed. More the number of electron donating substituent, more easily iron porphyrin will tend to lose the electron(s) at the ITIES [61].

Encouraged by these results, ET kinetics of iron porphyrin substituted with a range of electron accepting and donating groups was investigated by choosing the benzoquinone as a redox mediator. Dependence of the ET kinetics at the nitrobenzene-water ITIES of the porphyrins was envisaged using SECM. Both Butler-Volmer and Marcus inverted region ET kinetics were observed with the increase of low and high overpotentials as driving force, respectively [62]. We extended our study for the complex two-step electron transfer process, that is, zinc porphyrin substituted with the electron withdrawing groups. As expected, the oxidation potentials of the zinc porphyrin were positively shifted in the voltammograms recorded by TLCV. But, the ET kinetic data for the three different zinc porphyrin at the ITIES were not in line with the theoretical approximation [63]. Consecutive ET kinetics of zinc porphyrin was investigated by extending its  $\pi$ -conjugation using phenyl, naphthyl, and pyrenyl groups. ET rate estimated from the TLCV experiments were found to be slow if the substituted molecule is small and that of larger molecules was fast [64]. From the SECM experiments, it was revealed that, increase in the driving force lead to the slowdown of the ET rate. This was explained by taking the stereostructures of the molecules into consideration. The structure of the molecule has a dominating effect on the ET rate over that of Galvani potential of the ITIES [65].

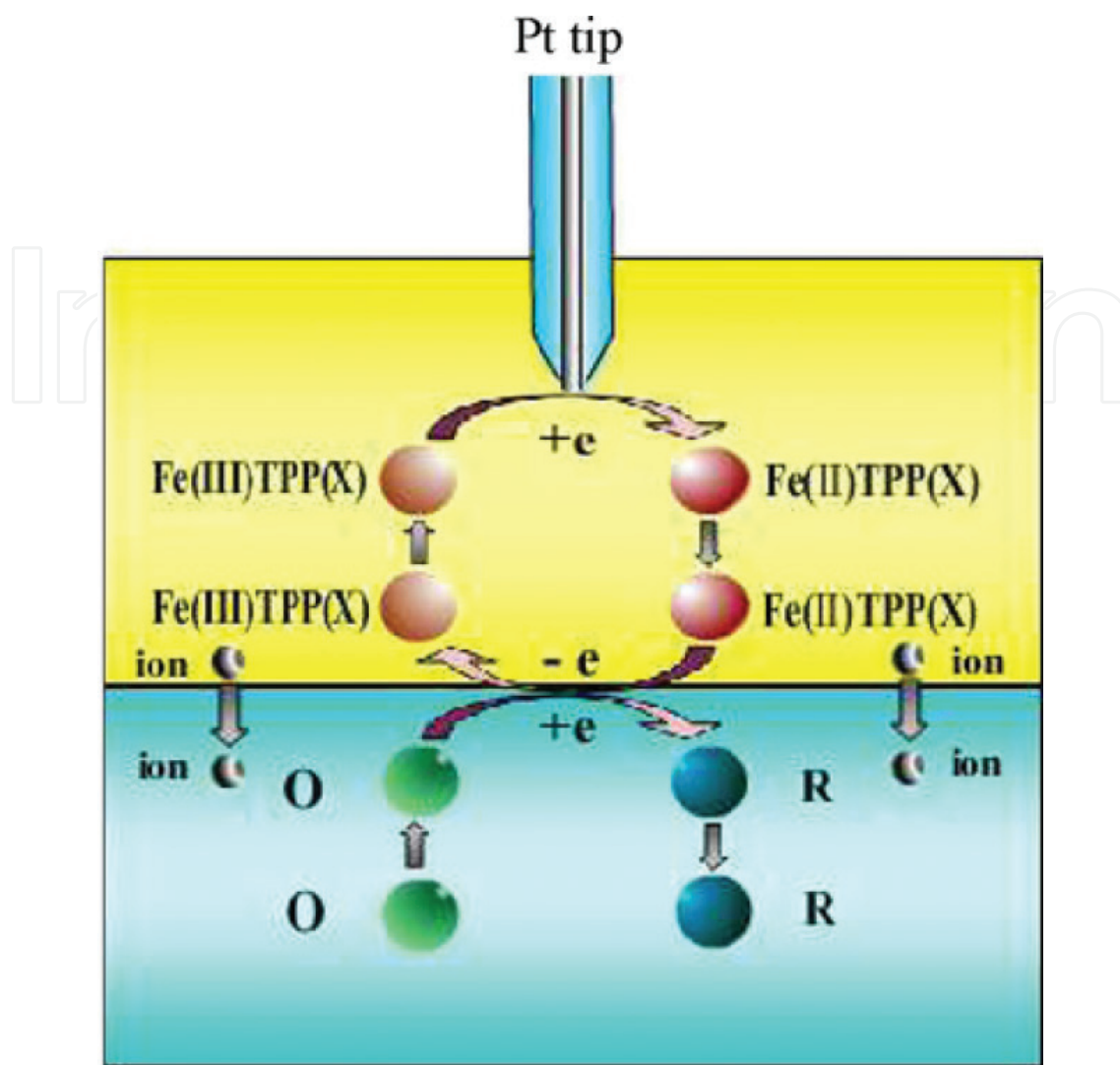


**Figure 6.** Schematic of the bimolecular redox reaction at the ITIES between the iron porphyrin taken in the nitrobenzene and  $[\text{Fe}(\text{CN})_6]^{3-}$  present in the aqueous phase. Reprinted from Ref. [61]. Copyright 2010 Elsevier Ltd.

## 6. Conclusions

Desired changes in the electronic properties of the porphyrin molecules achieved by tailoring the macrocyclic ring are investigated in detail using electrochemical techniques. Thiol-derivatized porphyrins are used to produce the self assembled monolayer (SAM) on the gold electrode to study their behavior at the solid/liquid interface. The SAMs composed of porphyrin molecules have been electrochemically investigated for the arrangement of molecules in it, imperfections and charge transfer across it. Simple and straightforward electrochemical methodologies have been developed to estimate the heterogeneous charge transfer constant at the solid/liquid and liquid/liquid interfaces using scanning electrochemical microscope (SECM). Porphyrin molecules have also been used in the electrochemical and electrochemiluminescence sensing applications.

## Author details

Xiaoquan Lu\* and Samrat Devaramani

\*Address all correspondence to: [luxq@nwnu.edu.cn](mailto:luxq@nwnu.edu.cn)

Key Laboratory of Bioelectrochemistry and Environmental Analysis of Gansu Province, College of Chemistry and Chemical Engineering, Northwest Normal University, Lanzhou, PR China

## References

- [1] Stéphanie D, Julien T, Valérie H. Multiporphyrinic cages: architectures and functions. *Chem. Rev.* 2014;**114**:8542–8578. doi:10.1021/cr400673y
- [2] Gema de la T, Giovanni B, Michael S, Anita H, Dirk MG, Tomas T. A voyage into the synthesis and photophysics of homo- and heterobinuclear ensembles of phthalocyanines and porphyrins. *Chem. Soc. Rev.* 2013;**42**:8049–8105. doi:10.1039/C3CS60140D
- [3] Chao H, Qingguo H, Changmin D, Liqi S, Defeng Z, Yanyan F, Huimin C, Jiangong C. Turn on fluorescence sensing of vapor phase electron donating amines via tetraphenylporphyrin or metallophenylporphyrin doped polyfluorene. *Chem. Commun.* 2010;**46**:7536–7538. doi:10.1039/C0CC01972K
- [4] Wallace WHW, Tony K, Doojin V, Chao Y, David JJ, Maxwell JC, Andrew BH. A porphyrin-hexa-peri-hexabenzocoronene-porphyrin triad: synthesis, photophysical properties and performance in a photovoltaic device. *J. Mater. Chem.* 2010;**20**:7005–7014. doi:10.1039/C0JM00311E
- [5] Karl MK, Eric VC. Electrochemistry of porphyrins and related macrocycles. *J. Solid State Electrochem.* 2003;**7**:254–258. doi:10.1007/s10008-002-0306-3
- [6] Ping C, Olga SF, Zhongping O, Sergei AV, Karl MK. Electrochemistry of platinum(II) porphyrins: effect of substituents and  $\pi$ -extension on redox potentials and site of electron transfer. *Inorg. Chem.* 2012;**51**:6200–6210. doi:10.1021/ic3003367
- [7] John AS, Xing-Zhi S, Jian-Guo M, Song-Ling J, Walter J, Craig JM, Craig JM. Nonplanar porphyrins and their significance in proteins. *Chem. Soc. Rev.* 1998;**27**:31–42. doi:10.1039/A827031Z
- [8] Karl MK, Erin VC, Guy R. Electrochemistry of metalloporphyrins in non-aqueous media. In: Karl M Kadish, Kevin MS, Roger G, editors. *The porphyrin handbook*, Vol 8. San Diego, CA: Academic Press; 2000, pp. 1–114
- [9] Kadish KM, Guy R, Erin VC, Gueletti L. Metalloporphyrins in nonaqueous media: database of redox potentials. In: Karl MK, Kevin MS, Roger G, editors. *The porphyrin handbook*, Vol 9. San Diego, CA: Academic Press; 2000, pp. 1–219

- [10] Fupeng Z, Xiaoquan L, Jiandong Y, Xiaoyan W, Hui S, Shaohua Z, Zhonghua X. Selective anion sensing through a self-assembled monolayer of thiol-end-functionalized porphyrin. *J. Phys. Chem. C*. 2009;**113**:13166–13172. doi:10.1021/jp9003278
- [11] Xiaoquan L, Dongxia Z, Zhenggen S, Bowan W, Bingzhang L, Xibin Z, Zhonghua X. A valuable visual colorimetric and electrochemical biosensor for porphyrin. *Biosensors Bioelectron*. 2011;**27**:172–177. doi:10.1016/j.bios.2011.06.043
- [12] Xiaoquan L, Yanli Q, Zhonghua X, Bowan W, Hetong Q, Dong L. Determination of explosives based on novel type of sensor using porphyrin functionalized carbon nanotubes. *Colloids Surf. B Biointerfaces*. 2011;**88**:396–401. doi:10.1016/j.colsurfb.2011.07.020
- [13] Yanli Q, Zhonghua X, Haicai S, Xibing Z, Jie D, Xiuhui L, Xiaoquan L. A high-performance and simple method for rapid and simultaneous determination of dihydroxybenzene isomers. *Analyst*. 2012;**137**:944–952. doi:10.1039/C1AN15945C
- [14] Yaqi H, Zhonghua X, Hongxia H, Ruixia A, Xiuhui L, Xiaoquan L. Photoelectrochemical sensing for hydroquinone based on porphyrin-functionalized Au nanoparticles on graphene. *Biosens. Bioelectron*. 2013;**47**:45–49. doi:10.1016/j.bios.2013.02.034
- [15] Xiaoquan L, Duoliang S, Jianmin Y, Baomei H, Xibin Z. Determination of m-dinitrobenzene based on novel type of sensor using thiol-porphyrin mixed monolayer-tethered polyaniline with intercalating fullerenols. *Talanta*. 2013;**115**:457–461. doi:10.1016/j.talanta.2013.06.002
- [16] Guofang Z, Xiuhui L, Jiandong Y, Xiujuan L, Xiaoquan L. Study of the adsorption kinetics of thiol-derivatized porphyrin on the surface of gold electrode. *J. Electroanal. Chem*. 2007;**605**:81–88. doi:10.1016/j.jelechem.2007.03.020
- [17] Xiaoquan L, Huiqing Y, Guofang Z, Jiandong Y. Study of the size and separation of pinholes in the self-assembled thiol-porphyrin monolayers on gold electrodes. *Thin Solid Films*. 2008;**516**:6476–6482. doi:10.1016/j.tsf.2008.02.036
- [18] James EH, Timothy AP, Chun-hsien C, Kevin WH, Roychelle SI, Wei O, Richard WL, Royce WM. Electrocatalytic activity of an immobilized cofacial diporphyrin depends on the electrode material. *Langmuir*. 1997;**13**:2143–2148. doi:10.1021/la960980u
- [19] Katsuaki S, Miwa T, Hiroshi F, Minoru S, Hiroshi S, Tetsuhiko Y, Kohei U. Formation and characterization of thiol-derivatized zinc (II) porphyrin monolayers on gold. *Thin Solid Films*. 1996;**273**:250–253. doi:10.1016/0040-6090(95)06790-6
- [20] Guofang Z, Huiqing Y, Jiandong Y, Ruixue Z, Xiaoquan L. Study of orientation mode of cobalt-porphyrin on the surface of gold electrode by electrocatalytic dioxygen reduction. *J. Mol. Catal. A Chem*. 2007;**269**:46–52. doi:10.1016/j.molcata.2006.11.041
- [21] Karl MK, Laurent F, Fabien B, Jean-Michel B, Claude PG, Roger G. Cobalt(IV) corroles as catalysts for the electroreduction of O<sub>2</sub>: reactions of heterobimetallic dyads containing a face-to-face linked Fe(III) or Mn(III) porphyrin. *J. Inorg. Biochem*. 2006;**100**:858–868. doi:10.1016/j.jinorgbio.2006.01.010



- [22] Christopher JC, Zhi-Heng L, Chunnian S, Fred CA, Daniel GN. Targeted proton delivery in the catalyzed reduction of oxygen to water by bimetallic pacman porphyrins. *J. Am. Chem. Soc.* 2004;**126**:10013–10020. doi:10.1021/ja049115j
- [23] Qin W, Fupeng Z, Wenting W, Xinghua X, Xiuhui L, Fanfu M, Yanyan S, Chen Y, Xiaoquan L. Direct electron transfer of thiol-derivatized tetraphenylporphyrin assembled on gold electrodes in an aqueous solution. *J. Phys. Chem. C.* 2009;**113**:9359–9367. doi:10.1021/jp803725x
- [24] Kin-ya T, Lianhe Y, Lingyun W, David FB, Jonathan SL. Synthesis of cyclic hexameric porphyrin arrays. Anchors for surface immobilization and columnar self-assembly. *J. Org. Chem.* 2003;**68**:8199–8207. doi:10.1021/jo034861c
- [25] Amir AY, Dennis S, Vladimir LM, Robert SL, Jonathan SL, Francisco Z, David FB. Characterization of self-assembled monolayers of porphyrins bearing multiple thiol-derivatized rigid-rod tethers. *J. Am. Chem. Soc.* 2004;**126**:11944–11953. doi:10.1021/ja047723t
- [26] Jiandong Y, Minrui L, Hongxiang L, Yanlian Y, Yoshiaki K, Chen W, Keiichi T, Xiaoquan L, Wenping H. Characterization and application of self-assembly porphyrin with four “clips” on gold surface. *J. Phys. Chem. C.* 2010;**114**:12320–12324. doi:10.1021/jp1020643
- [27] Yan Z, Xiaoquan L, Tianlu L, Yina C, Xiuhui L, Limin Z. Studies on interaction of porphyrin and its complexes with DNA at interface on gold electrode modified by thiol-porphyrin self-assembled monolayer. *J. Solid State Electrochem.* 2007;**11**:1303–1312. doi:10.1007/s10008-007-0291-7
- [28] Shen-Ming C, Sz-Vin C. The interaction of water-soluble iron porphyrins with DNA films and the electrocatalytic properties for inorganic and organic nitro compounds. *Electrochim. Acta.* 2003;**48**:4049–4069. doi:10.1016/S0013-4686(03)00562-0
- [29] Xiaoquan L, Fupeng Z, Hui S, Xiaoyan W, Zhonghua X. Investigation of the electrochemical behavior of multilayers film assembled porphyrin/gold nanoparticles on gold electrode. *Electrochim. Acta.* 2010;**55**:3634–3642. doi:10.1016/j.electacta.2009.11.004
- [30] Fardad F, Allen JB, Michael VM. Voltammetric and scanning electrochemical microscopic studies of the adsorption kinetics and self-assembly of *n*-alkanethiol monolayers on gold. *Isr. J. Chem.* 1997;**37**:155–163. doi:10.1002/ijch.199700019
- [31] Céline C, Frédéric K, Allen JB. Cyclic voltammetric and scanning electrochemical microscopic study of menadione permeability through a self-assembled monolayer on a gold electrode. *Langmuir.* 2002;**18**:8134–8141. doi:10.1021/la0258906
- [32] Jalal G, Fanny H, Bruno F, Philippe H. Scanning electrochemical microscopy investigations of monolayers bound to p-type silicon substrates. *Anal. Chem.* 2006;**78**:6019–6025. doi:10.1021/ac060058h
- [33] Xiaoquan L, Limin Z, Minrui L, Xiaoqiang W, Yan Z, Xiuhui L, Guofang Z. Electrochemical characterization of self-assembled thiol-porphyrin monolayers on gold electrodes by SECM. *Chem. Phys. Chem.* 2006;**7**:854–862. doi:10.1002/cphc.200500492



- [34] Biao L, Allen JB, Michael VM, Stephen E. Creager. Electron transfer at self-assembled monolayers measured by scanning electrochemical microscopy. *J. Am. Chem. Soc.* 2004;**126**:1485–1492. doi:10.1021/ja038611p
- [35] Wenting W, Xiujuan L, Xiaoyan W, Hui S, Xiuhui L, Xiaoquan L. Comparative electrochemical behaviors of a series of SH-terminated-functionalized porphyrins assembled on a gold electrode by scanning electrochemical microscopy (SECM). *J. Phys. Chem. B.* 2010;**114**:10436–10441. doi:10.1021/jp1026064
- [36] Wenting W, Yaqi H, Chunming W, Xiaoquan L. Comparative electrochemical investigations on series of SH-terminated-functional porphyrins. *Electrochim. Acta.* 2012;**65**:244–250. doi:10.1016/j.electacta.2012.01.049
- [37] Yann L, Delphine S, Laurent R, Philippe H. SECM investigations of immobilized porphyrins films. *Langmuir.* 2010;**26**:14983–14989. doi:10.1021/la101294s
- [38] Mary EW, Joseph TH. Scanning electrochemical microscopy assessment of rates of molecular transport through mesoporous thin-films of porphyrinic “molecular squares”. *J. Phys. Chem. B.* 2001;**105**:8944–8950. doi:10.1021/jp010881b
- [39] Zhonghua X, Hetong Q, Jie D, Bowan W, Xiuhui L, Xiaoquan L, Xibin Z. A novel method to remove self-assembled monolayer of porphyrin from the gold surface by cyclic voltammetry. *J. Adhesion Sci. Technol.* 2012;**26**:1521–1529. doi:10.1163/156856111X618371
- [40] Wenting W, Duoliang S, Yong Y, Chunming W, Yaqi H, Xiaoquan L. A novel method for dynamic investigations of photoinduced electron transport using functionalized-porphyrin at ITO/liquid interface. *Chem. Commun.* 2011;**47**:6975–6977. doi:10.1039/c1cc10842e
- [41] Michael VM. Theory. In: Allen JB, Michael VM, editors. *Scanning electrochemical microscopy*. New York: Marcel Dekker; 2001, pp. 145–199
- [42] Xiaoquan L, Yaqi H, Wenting W, Jie D, Hongxia H, Ruixia A, Xiuhui L. A novel platform to study the photoinduced electron transfer at a dye-sensitized solid/liquid interface. *Colloids Surf. B Biointerfaces.* 2013;**103**:608–614. doi:10.1016/j.colsurfb.2012.11.013
- [43] Xingming N, Liang M, Shouting Z, Dongdong Q, Duoliang S, Yaqi H, Xiaoquan L. Construction of a porphyrin-based nanohybrid as an analogue of chlorophyll protein complexes and its light-harvesting behavior research. *Phys. Chem. C.* 2016;**120**:919–926. doi:10.1021/acs.jpcc.5b11246
- [44] Yuan J, Dong-Dong Q, Yan-Ru F, Hui-Xia G, Shi-Xia W, Xingming N, Xiaoquan L. Investigation of photoinduced electron transfer on TiO<sub>2</sub> nanowire arrays/porphyrin composite via scanning electrochemical microscopy. *RSC Adv.* 2015;**5**:56697–56703. doi:10.1039/c5ra08485g
- [45] Mark MR. Electrochemiluminescence (ECL). *Chem. Rev.* 2004;**104**:3003–3036. doi:10.1021/cr020373d
- [46] Lianzhe H, Guobao X. Applications and trends in electrochemiluminescence. *Chem. Soc. Rev.* 2010;**39**:3275–3304. doi:10.1039/b923679c

- [47] Toby RL, Mark MR. Electrogenated chemiluminescence of the platinum (II) octa-ethylporphyrin/tri-n-propylamine system. *Inorg. Chim. Acta.* 2005;**358**:2141–2145. doi:10.1016/j.ica.2004.12.017
- [48] Israel R, Allen JB. Electrogenated chemiluminescence. 37. Aqueous ecl systems based on  $\text{ru}(2,2'\text{-bip~ridine})_3^{2+}$  and oxalate or organic acids. *J. Am. Chem. Soc.* 1981;**103**:512–516. doi:10.1021/ja00401a031
- [49] Fang-Chung C, Jinn-Hsuan H, Chin-Yu C, Oliver SY, Tong-Ing H. Electrogenated chemiluminescence of sterically hindered porphyrins in aqueous media. *J. Electroanal. Chem.* 2001;**499**:17–23. doi:10.1016/S0022-0728(00)00439-3
- [50] Jing Z, Samrat D, Duoliang S, Xiaoquan L. Electrochemiluminescence behavior of meso-tetra (4-sulfonatophenyl)porphyrin in aqueous medium: its application for highly selective sensing of nanomolar  $\text{Cu}^{2+}$ . *Anal. Bioanal. Chem.* 2016;**408**:7155–7163. doi:10.1007/s00216-016-9655-0
- [51] Di L, Baomei H, Li W, Ahmed M, Shixia W, Xiaoquan L. Cathodic electrochemiluminescence of meso-tetra(4-carboxyphenyl) porphyrin/potassium peroxydisulfate system in aqueous media. *Electrochim. Acta.* 2015;**151**:42–49. doi:10.1007/s00216-016-9655-0
- [52] Canty P, Väre L, Håkansson M, Spehar AM, Papkovsky D, Ala-Kleme T, Kankare J, Kulmala S. Time-resolved electrochemiluminescence of platinum(II) coproporphyrin. *Anal. Chim. Acta.* 2002;**453**:269–279. doi:10.1016/S0003-2670(01)01413-1
- [53] Angela B, Mark MR. Coreactant electrogenerated chemiluminescence of ruthenium porphyrins. *Inorg. Chim. Acta.* 2009;**362**:1974–1976. doi:10.1016/j.ica.2008.09.022
- [54] Guang-Yao Z, Sheng-Yuan D, Xue-Ji Z, Dan S. Cathodic electrochemiluminescence of singlet oxygen induced by the electroactive zinc porphyrin in aqueous media. *Electrochim. Acta.* 2016;**190**:64–68. doi:10.1016/j.electacta.2015.12.228
- [55] Shengyuan D, Tingting Z, Xubo J, Ying W, Peng X, Dan S, Xueji Z. Detection of zinc finger protein (EGR1) based on electrogenerated chemiluminescence from singlet oxygen produced in a nanoclay-supported porphyrin environment. *Anal. Chem.* 2015;**87**:9155–9162. doi:10.1021/acs.analchem.5b01318
- [56] Shengyuan D, Peixin Y, Xubo J, Dan S, Xueji Z. Carbon nitride nanosheet-supported porphyrin: a new biomimetic catalyst for highly efficient bioanalysis. *ACS Appl. Mater. Interfaces.* 2015;**7**:543–552. doi:10.1021/am506645h
- [57] Li W, Jiasi W, Lingyan F, Jinsong R, Weili W, Xiaogang Q. Label-free ultrasensitive detection of human telomerase activity using porphyrin-functionalized graphene and electrochemiluminescence technique. *Adv. Mater.* 2012;**24**:2447–2452. doi:10.1002/adma.201200412
- [58] Pekka P, Hubert HG. Liquid/liquid interfaces, electrochemistry at. *Encyclopedia of analytical chemistry.* New Jersey: John Wiley & Sons, Ltd; 2006–2012.
- [59] Biao L, Michael VM. Potential-independent electron transfer rate at the liquid/liquid interface. *J. Am. Chem. Soc.* 1999;**121**:8352–8355. doi:10.1021/jp013543j

- [60] Xiaoquan L, Ping S, Dongna Y, Bowan W, Zhonghua X, Xibing Z, Ruiping S, Li L, Xiuhui L. Heterogeneous consecutive electron transfer at graphite electrodes under steady state. *Anal. Chem.* 2010;**82**:8598–8603. doi:10.1021/ac1016997
- [61] Xiaoquan L, Junying M, Ruiping S, Mina N, Fanfu M, Jie D, Xiaoyan W, Hui S. Substituent effects of iron porphyrins: structural, kinetic, and theoretical studies. *Electrochim. Acta.* 2010;**56**:251–256. doi:10.1016/j.electacta.2010.08.088
- [62] Xiaoquan L, Wenting G, Ruiping S, Xiuhui L. Investigation of electrochemical properties of metalloporphyrin species at the liquid/liquid interface by switching substitutes on the porphyrin ring. *Electroanalysis.* 2012;**24**:2341–2347. doi:10.1002/elan.201200396
- [63] Xiaoquan L, Yao L, Ping S, Bowan W, Zhonghua X, Xiuhui L, Xibing Z. Investigation of the consecutive electron transfer of metalloporphyrin species containing different substituents at the liquid/liquid interface by thin-layer cyclic voltammetry. *J. Phys. Chem. C.* 2012;**116**:16660–16665. doi:10.1021/jp3061043
- [64] Yanru F, Yu H, Shixia W, Yuan J, Duoliang S, Xiaoquan L. Investigation of interfacial consecutive electron transfer and redox behaviors of zinc-tetraarylporphyrins. *Electrochim. Acta.* 2016;**190**:419–425. doi:10.1016/j.electacta.2015.12.167
- [65] Yanru Fan, Yu Huang, Yuan Jiang, Xingming Ning, Xuemei Wang, Duoliang Shan, Xiaoquan Lu. Comparative study on the interfacial electron transfer of zinc porphyrins with meso-p-extension at a 2<sup>n</sup> pattern. *J. Colloid Interface Sci.* 2016;**462**:100–109. doi:10.1016/j.jcis.2015.09.063